advances
in radiation oncology

Scientific Article

Exploring the Use of Contour-Based Intrafraction Motion Review for Spine Stereotactic Body Radiation Therapy Treatments

Erika A. Jank,* and Ashley J. Cetnar, PhD

Department of Radiation Oncology, The Ohio State University Wexner Medical Center, Columbus, Ohio

Purpose: Patient motion during radiation therapy treatment is a concern, especially for spine stereotactic body radiation therapy cases where the sharper dose gradient presents a toxicity threat to the spinal cord. Intrafraction motion review (IMR) is an application used to monitor patient position during treatment. The presence of spinal fixation hardware presents an opportunity for motion tracking to manually pause the beam.

Methods and Materials: A cohort of 17 clinicians were shown a video of the imaging console during a simulated treatment. Participants decided after each triggered image if they would pause the treatment beam, indicating that they believed the phantom to have moved outside of clinical tolerance. A spine phantom with hardware intact was positioned on a motion platform, which was programmed to make shifts ranging in size from 0.5 to 1.5 mm. A 1-mm isotropic expansion contour from the hardware was overlaid on the triggered planar x-ray images using the IMR application.

Results: User perception sensitivity did not exceed 0.5 until there was a physical shift of 1.4 mm, indicating that most users will not be able to reliably discriminate submillimeter shifts using contour-based shift identification.

Conclusions: If adaptations to standard of care are implemented clinically, the proposed method should be evaluated and the role of training and education should be examined before implementation. However, contour-based IMR could still provide beneficial information for larger intrafraction motion during treatment and could be valuable for identifying gross anatomic motion during treatment.

Introduction

Spinal metastases occur in about 40% of patients with cancer.[1] As with most forms of cancer, treatment modalities include surgery, chemotherapy, radiation therapy (RT), or a combination of these options. Because of the proximity and radiosensitive nature of the spinal cord,

precision and accuracy in RT are of great importance in the treatment of spinal metastases.[2] Therefore, the use of stereotactic body RT (SBRT) is a preferred method of care for these patients because a sharper dose gradient is achievable with fewer treatment fractions.[3] In addition to fewer fractions for the patient, radiation toxicity has decreased and the survival rate has increased with the implementation of spine SBRT.[4]

Metastases in the spinal column often cause cord compression, leading to instability, pain, and various neurologic issues.[5] Avoiding malignant spinal cord compression typically requires the surgical implantation of hardware designed for decompression, followed by RT.[1,6] With screw-rod implementation, the goal of the

*Corresponding author: Erika A. Jank; E-mail: erikajank@creighton.edu

hardware is to fixate the spine. For patients who receive spinal hardware insertion, a secondary advantage is presented in that it can also be used as a surrogate for localization and monitoring during RT. The screw-rod fixation device is commonly made of titanium,[5] which is visualized in striking contrast on x-ray−based imaging. Hence, there is a potential opportunity to track this hardware device during the RT treatment process.

Motion during treatment is a concern with patients receiving spine SBRT because of the proximity of the spinal cord as an organ at risk and the high dose per fraction being delivered where radiation-induced myelopathy can occur as an effect of hypofractionated RT.[6] To monitor and manage movement while the beam is on, there are multiple options to consider. Treatment systems such as the CyberKnife (Accuray, Sunnyvale, CA) and ExacTrac (Elekta, Stockholm, Sweden) use in-room kV x-ray orthogonal imaging systems to track motion and offer the ability for 6-dimensional intrafraction corrections.[7,8] As an alternative to these existing systems, intrafraction motion review (IMR) is an application for Advanced Motion Management (version 2.7) on the Truebeam (Varian, Palo Alto, CA) that allows for real-time monitoring of patient position during treatment.

IMR is implemented clinically through the utilization of Truebeam's on-board imager (OBI) to capture kV images during treatment triggered by time, gantry angle, or monitor units.[9] Fiducial markers can be detected in the triggered images and monitored in real time for comparison between expected and actual locations. This information can be used to determine whether patient readjustment is clinically necessary[9] and has been used for disease sites such as the prostate and spine.[2,9] IMR implementation for spinal cases has been documented by Moffitt Cancer Center, where the movement of vertebral bodies was monitored,[2] with results indicating patient motion can go unnoticed if only the targeted vertebra is contoured and not the surrounding structures. The feasibility of implementing a contour-based approach for monitoring SBRT patients with spinal hardware has been demonstrated clinically.[10] In this study, the feasibility of using IMR for spinal SBRT cases with hardware was evaluated through a phantom study, focusing on quantifying the tolerance of shifts that can be detected by clinical users.

Methods and Materials

To explore the detectability of shifts and the realistic utilization of IMR in a clinical setting, 2 types of simulated treatments were developed (Fig. 1). The first type, or phase 1, consisted of arc-based treatment plans. For arc 1 of treatment plan 1, the gantry delivered a full arc rotating in the clockwise direction with displacement values of the motion phantom randomized between 0.5 and 1.5 mm shifts. For arc 2 of treatment plan 1, the gantry rotated in the counterclockwise direction and the motion phantom displacement values were replicated from the values generated for arc 1, but in reverse order, mirroring the first arc to test observer reproducibility.

The QUASAR Heavy Duty Programmable Respiratory Motion Platform (Modus QA, London, Canada) was used to simulate intrafraction patient motion. Tab delimited files were developed to control the phantom specifying the time and displacement. The phantom was programmed to move in 1 dimension (superior/inferior). Integers were generated using Microsoft Excel's RANDBETWEEN function to include values representing shifts between 0.5 and 1.5 mm in magnitude. These are clinically relevant values that were used to simulate random patient movements that can potentially occur during SBRT spine treatment. The range was determined to understand the precision of the user observation because the contour for the observer is a 1- mm expansion from the hardware. To synchronize the movement of the motion platform with the intrafraction imaging, the time trigger was used to acquire kV images every 5 seconds such that the movement of the platform occurred between image acquisitions.

Because the motion phantom positions were randomly generated for the first part, the second part of phase 1 was developed to better understand potential limitations due to angular dependance. Treatment plan 2 used the logic that if the displacement was greater than 1 mm for that gantry angle in the first plan, a number between 0.5 and 1 mm should be generated at this timepoint, and if the displacement was less than 1 mm for that gantry angle in the first plan then a number between 1 and 1.5 mm should be generated. For arc 4 of treatment plan 2, the gantry rotated in the counterclockwise direction and the motion phantom displacement values were the values generated for arc 3 but in the reverse order to test observer reproducibility.

Phase 2 consisted of linear stepwise motion in increments of 0.1 mm, starting from the center position and moving slowly to a displacement value of 1.5 mm to reduce the angular variable. This method was conducted at 2 stationary gantry angles of 0° and 90° to test for shift detectability. Figure 1 depicts a visual representation of the 6 individual video clips for the simulated treatment shown to each participant.

A planning computed tomography (CT) was obtained and reconstructed using metal artifact reduction with 1.25-mm slice thickness. The spinal hardware was imported to Eclipse (Varian) and contoured with the bone window and level, and a 1-mm isotropic expansion contour was created from the hardware contour. Test plans were generated in Eclipse for use at the console to deliver the arc and static plans. To set up the simulated treatment, a spine phantom with titanium screw-rod hardware was arranged on top of the QUASAR motion platform, representing the orientation of the device in the prone position. This is illustrated in Fig. 2A and B.
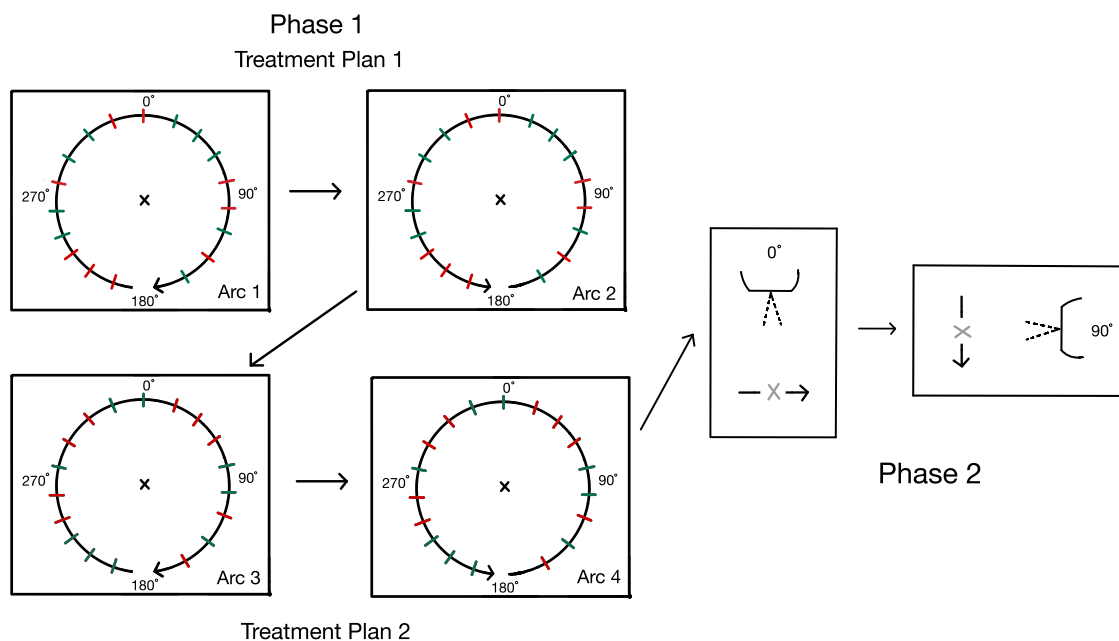
Figure 1   Diagram of the set-up for treatment plans 1 and 2 in phase 1 and phase 2 of the stimulated treatment. This demonstrates the angular position of the gantry and shows the pattern of shift displacements, with a red dash representing a shift with magnitude 1 to 1.5 mm and a green dash representing a 0.5- to 0.9-mm shift.

Before the start of treatment, a cone beam CT was performed to match the alignment of the spinal hardware phantom with its planning CT position. Shifts were performed and verified with a cone beam CT and kV pair. After necessary adjustments were made, kV imaging during treatment was added to the plan on the treatment console. The images were selected to be triggered in 5-second intervals. After this step, the treatment plans were delivered while the software that controlled the phantom

Figure 2   Set-up of the simulated treatment with the QUASAR motion platform beneath the spine hardware phantom. 4K pass-through capture card was connected to the treatment console to achieve a high-definition recording of the simulated treatment.

was synchronized by starting the motion at the display of the first triggered image.

To record the console display during the simulated treatment, a 4K pass-through capture card (AVerMedia, New Taipei City, Taiwan) was used, allowing for a high-definition recording of the treatment console. This recording was used to obtain observational data for the cohort of participants in this study. The capture card is shown and the setup is illustrated in Fig. 2.

Participants were recruited through an e-mail invitation sent to physicists, physicians, and therapists in the department. Participants were scheduled for a 15-minute session with the researcher. During each session, participants were asked about their role within the radiation oncology department. Then, the same educational information about the study was conveyed to each user before watching the simulated treatments. This information included a brief description of each phase and a general overview of the recorded video the participants would view. The size of the contour was also stated, as well as the instructions on how to indicate their choice to pause treatment or not. With phase 1, participants verbally indicated if they would pause or continue treatment for each triggered image. This was followed by phase 2, where users paused the video when they believed the phantom to have shifted outside of clinical tolerance. Data were collected and analyzed using Microsoft Excel.

A true positive in the context of this study is defined as the occurrence of a shift of 1 mm or greater and the user choosing to pause treatment as expected. A true negative in the context of this study is defined as an event when the

physical shift was less than 1 mm in magnitude and the user chose to continue treatment as expected. A false negative implies that a shift of 1 mm or greater occurred, but the user chose to continue treatment. Likewise, a false positive implies that a user paused treatment even though the shift was less than 1 mm in magnitude. In each simulated treatment, an individual user had 4 (N = 4) opportunities at each gantry angle to decide on whether to pause the beam or not. The accuracy of each decision was determined in a binary fashion. One indicated that the user chose to pause the beam and the shift was greater than or equal to 1 mm in magnitude or that they chose to continue the beam and the shift was less than 1 mm. Zero indicated that the user chose to pause the beam and the shift was less than 1 mm or that they chose to continue the beam and the shift was greater than or equal to 1 mm in magnitude.

Results

A cohort of 17 individuals within the radiation oncology department at Ohio State University were involved in this study. Demographic data were recorded for the role of each participant in radiation oncology. Each treatment arc began with gantry positioned at 180° (kV imaging source at 90°) and motion phantom at centered home position. Figure 3 depicts the overall user accuracy based on phantom displacement from the center position between 0.5 and 1.5 mm. These results indicate that the highest percent inaccuracy is associated with 1- and 1.1-mm shifts, respectively 69% and 71%. When considering shifts of magnitude less than 1 mm (0.5-0.9 mm), accuracy was greater than 90% for all. When considering shifts of magnitude greater than or equal to 1 mm (1-1.5 mm), accuracy was above 60% only for 1.4 and 1.5 mm shifts. The highest percent accuracy occurred with 1.4-mm shifts when comparing shifts that were greater than or equal to 1 mm. Additionally, user perception sensitivity did not exceed 0.5 until a 1.4-mm shift occurred.
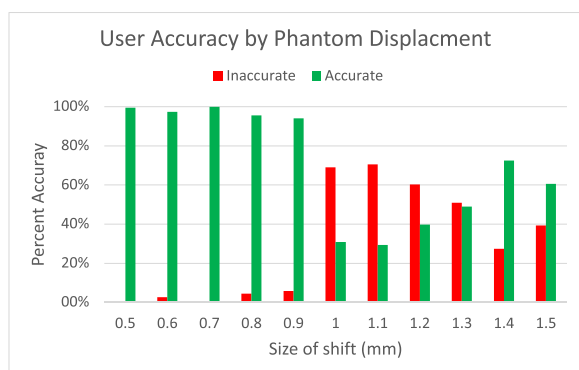

Figure 3 The percent accuracy and inaccuracy of users in their decision to pause or continue treatment at each magnitude of phantom displacement.

Next, the user detection accuracy was compared between the 3 roles of individuals within the radiation oncology department. The cohort consisted of 11 physicists, 3 physicians, and 3 therapists. Overall, the percent accuracy was comparable between physicists, physicians, and therapists. It was determined that there is no statistically significant difference in accuracy between the 3 roles based on the Kruskal-Wallis test ($P = .921$).

The accuracy of individuals correctly determining whether the item was in or out of tolerance can also be related to the angle of the OBI. Figure 4 demonstrates how the overall accuracy may exhibit angular dependance of image acquisition. Each user had 2 opportunities to observe the phantom in a position less than 1-mm away from its home position and 2 opportunities to observe the phantom in a position greater than or equal to 1 mm in each gantry angle bin. One hundred percent accuracy would be associated with an accuracy count of 68 within an angular segment. The highest accuracy count achieved at any given angle in this study coincided with an OBI angle of 180° (92.6%), and the lowest occurred at 145° (50%).

Confusion matrix elements were calculated using the data extracted from this study including the true positive, true negative, false positive, and false negative parameters. Figure 5 summarizes these findings and compares them with accuracy for each imaging projection path or segment. One segment refers to 2 angular positions of the OBI, representing a specific point in the arc of motion and its complementary angle because data are redundant upon the path. Segment 1 refers to the angle pair of 0°/180°, as seen by the light green color in the pie chart in Fig. 5. The angle pair associated with each subsequent segment is noted in the following sections and represented by 2 wedges of the same color in the circle on the top right of Fig. 5. The segment associated with the highest accuracy was segment 2, and lowest accuracy occurred at segment 8. The segment associated with the most true positives was segment 1, and the least amount was seen at segment 6. These data are consistent with the findings displayed in Fig. 4, with the highest accuracy occurring at angles at or near 180°, corresponding to segments 1 and 2. The most false positives occurred with segment 7 and the most false negatives occurred with segment 8, coinciding with the lowest accuracy occurring at segment 8 or the angle pair of 145°/325°.

Another parameter used to analyze the data from this study was an intrauser comparison used to test reliability. Treatment plan 1 consisted of arcs 1 and 2, both having the same randomized displacement values but in the opposite orders. Therefore, the reliability of a user identifying the shift of a specific magnitude consistently at 2 different timepoints could be determined. Likewise, treatment plan 2 consisted of arc 3 and 4, which were constructed with the same methodology, so there were 36 possible chances for evaluating internal consistency of each user. In this way, perfect consistency would be a
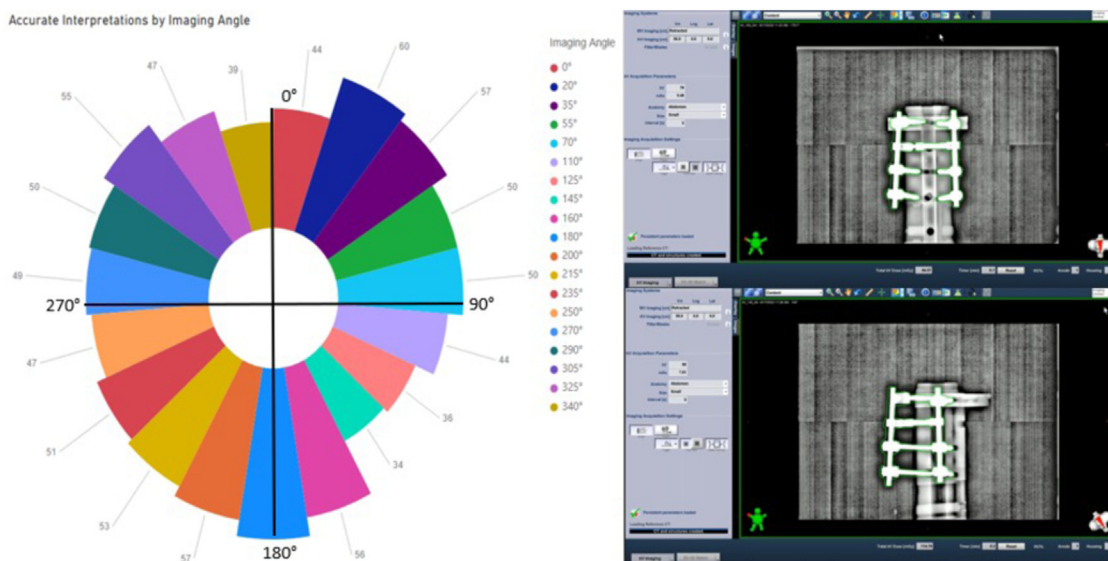
Figure 4 The aster plot depicts the number of accurate interpretations of all shifts occurring at specific imaging angles. The top right shows the treatment console during image acquisition at 180° and the bottom right shows this at 145°, corresponding to the imaging angles with the most and least counts of accuracy. Both frames show examples of the phantom within the 1-mm clinical threshold contour.

score of 36 and perfect accuracy would be a score of 80. Figure 6 demonstrates the correlation between consistency and accuracy of users. The users are listed in order from highest to lowest accuracy. The correlation coefficient between the 2 variables was calculated to be −0.54, meaning that there is a moderate negative correlation between accuracy and consistency.

When comparing the accuracy associated with each arc, it was determined that arc 4 of 4 was the most accurate across all users when analyzing the 2 arc-based treatment plans. The average user accuracy by arc increased 12% between arc 1 and 4.

For phase 2 of this study, individuals were shown a video of the phantom slowly shifting out of clinical
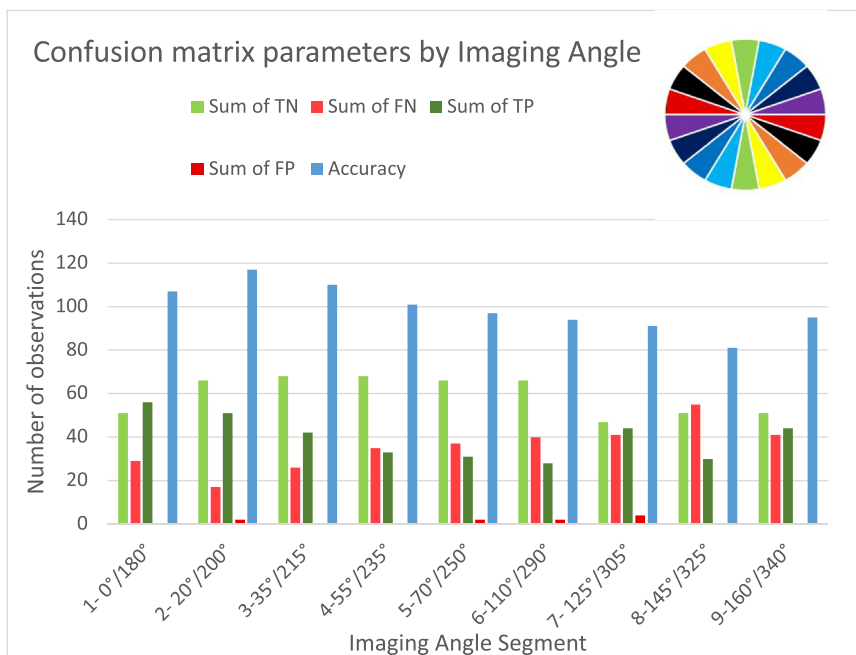
Figure 5 The number of true negatives, false negatives, true positives, false positives, and counts of accuracy for each of the 9 segments. Each segment is represented by a single color on the pie chart in the top right, with the complementary imaging angles displayed in the correct physical locations.
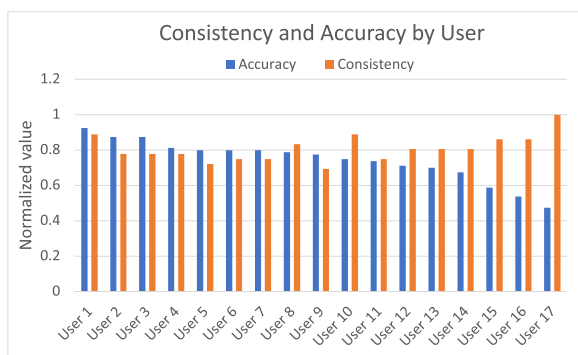
Figure 6 The normalized consistency and accuracy of each user.

tolerance, and users were asked to indicate when they believed the phantom hardware to have exited this tolerance. Figure 7 compares the magnitude of the phantom's shift when the beam was paused by each user at the 2 static field treatment angles. The static field treatment at 0° was shown first, and the treatment at a gantry angle of 90° was shown second. The range of size of shift was the same for both angles, but the average value that the video was paused at was 1.4 mm for 0° and 1.3 mm for 90°.

Discussion

This study tests the accuracy of clinical users in detecting intrafraction motion using triggered kV images of spinal hardware during simulated treatment scenarios. Although titanium-based screw-rod fixation devices are primarily used to stabilize the spinal column, we have found they can also be used as a surrogate for localization.[10] The Hounsfield unit of titanium is approximately 3 times greater than that of bone, providing high contrast to aid in visualization of potential motion compared with vertebral bodies. The cause of inaccuracy in recognizing
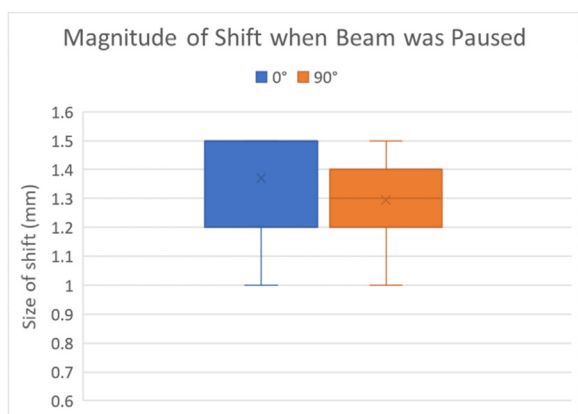
Figure 7 The range and mean of the magnitude of the phantom's shift when users chose to pause the treatment beam during the 2 static-field treatments of phase 2.

shifts can be attributed to numerous factors, but this research examined the ability of the clinical user to visually detect shifts of various magnitudes during simulated treatments.

Because of the high accuracy of users correctly continuing treatment with shifts less than 1 mm in magnitude, it can be concluded that individuals in the study were proficient in accurately detecting shifts occurring within clinical tolerance. But, over 2/3 of users had difficulty detecting shifts of magnitude 1 and 1.1 mm in size. Within the setup of this phantom study, a 1-mm shift was not reliably detected by the human eye for a majority of the users. Therefore, it should be reconsidered how contour-based IMR is used in clinical workflows to more accurately monitor patient position.

Overall, as the magnitude of displacement increased, detection accuracy increased, but it never exceeded 75% for even the largest shifts (1.3, 1.4, and 1.5 mm) used in this study. The use of a 1-mm isotropic contour has not shown to be a reliable metric to use when monitoring submillimeter intrafraction motion introduced in this study. The largest change in accuracy occurred between 1.3- and 1.4-mm magnitude displacements, increasing from 49% to 73%, respectively. A smaller isotropic contour could potentially be used as the overlay on the triggered kV images so that shifts closer to the 1-mm threshold are detected as "out," but this was not evaluated in the scope of this study. For future studies, the size of the contour could be an experimental variable for seeking to improve the detection accuracy of shifts at the desired clinical threshold.

There is also a large range in percent accuracy between users, indicating user variability. Additionally, the last arc shown to individuals in this study correlated to the arc with the highest percent accuracy. Given these findings, it can be suggested that training and education could play a role in improving the overall detection accuracy of clinical users. For future studies, scores from users before and after training could be compared to determine the role of education as a factor in improving accuracy on an individual level.

With shifts greater than or equal to 1 mm in magnitude, an accuracy of 100% was not reached with any magnitude shift in this study. As seen in Fig. 3, the shift with highest associated accuracy was 1.4 mm in magnitude. The most 1.4-mm shifts occurred at segment 2 (20°/200° angle pair), which was also the segment that had the highest accuracy. After extrapolating the data for shifts greater than or equal to 1 mm in magnitude, it was projected that at shifts around the 2-mm mark, accuracy in correct detection would approach 100%. Expanding the range in the size of shifts to reach percent accuracies near 100% could be explored in future work.

Based on Fig. 4, the angles associated with the highest accuracy are clustered around 20° and 180°. The familiarity of interpreting images at these cardinal angles could account for the increase in accuracy. The lowest accuracy

occurred at 145°, which was associated with approximately half of the accuracy achieved for 180°. Because of differences in reported accuracy with imaging angle, the detectability of shifts by users could have angular dependence. This discovery is consistent with the findings in Fig. 5, showing how the count of true positives, true negatives, false positives, false negatives, and accuracy changes as a result of the imaging angle segment.

Overall, there were very few false positives, supporting user proficiency with determining shifts less than 1 mm in magnitude to be within clinical tolerance. There is a trend showing the rate of false negatives to be low, indicating the greatest source of inaccuracy was associated with shifts being called "in tolerance" when the displacements exceeded clinical tolerance. Based on the correlation coefficient between accuracy and consistency, there is a moderate negative correlation between these 2 variables, as seen in Fig. 6. Illustrated by the right side of the bar graph, consistency increased as accuracy decreased. This trend indicates that high consistency does not always equate to high accuracy. Demonstrated by the data for user 17, this individual was perfectly consistent but had the lowest overall accuracy.

In phase 2, the simulated treatment with the gantry positioned at 0° (OBI at 270°) was shown before the video with the gantry at 90° (OBI at 0°). Most users were more accurate with pausing the beam closer to the 1-mm clinical threshold with the video where the gantry was at 90°. This decrease in tolerance could indicate that users learned from the first static field treatment video and were more accurate because of this previous experience. Seventy-six percent of users altered their response between the first and second videos, with only 15% of those individuals increasing their tolerance. This overall decrease in tolerance further indicates the role of training and education to possibly improve user accuracy for IMR, showing that familiarity with the application can improve accuracy in detection. An outside study discovered that movement was more difficult to detect if the OBI and shift vector were parallel. Further investigation could be pursued by randomizing the order of the videos to identify if the difference was due to angular dependence or users learning during the study, and experimentation with additional angles could also be incorporated.

The vigilance decrement function is the psychological concept of performance degradation in situations in which individuals must pay attention to a singular thing for an extended period of time.[11] The effects of this concept could have influenced the results of this study given the requirement for participants to focus on noticing small shifts for multiple minutes at a time. Incorporating the speed of the simulated treatments as an experimental variable could be explored in future work. This phenomenon could have had the most noticeable effect on phase 2 results, where the phantom was slowly drifting from its home position to the maximum displacement of 1.5 mm

in the span of 90 seconds. Computer-based algorithms have been implemented for the tracking and monitoring of individual markers[9,12,13] with single-images, and other technologies have implemented orthogonal kV imaging techniques to minimize the human factors when analyzing imaging data during treatment. Commercial systems identifying fiducial bone markers or vertebral bodies have reported submillimeter accuracy in phantom studies.[8,14] Although this study focused on observer difference, the role of computer-assisted decision-making could increase accuracy for patients with spinal hardware in the future.

Another constraint of this study is the limit on accuracy of the 1-mm isotropic expansion contour in 3-dimensional space. Because of the 1.25-mm slice thickness of the planning CT, the interpolation algorithm of Eclipse does not have an infinitesimal amount of data points to create a 1-mm isotropic expansion contour from the hardware contour. The resolution of this system presents a source of uncertainty in that the generated expansion contour could be slightly greater than 1 mm in certain directions within 3-dimensional space. Therefore, the inherent software restriction on accuracy due to voxel resolution and inaccurate contour generation is recognized as a limitation to this study. Instead of creating an isotropic expansion of the entire hardware structure, specific regions of interest, such as limiting the structure to the vertical and horizontal stabilization rods, could be used to standardize decision-making because the inclusion of the individual pedicle screws may be more challenging to interpret because of their complex geometry.

Additional limitations to this study include that the QUASAR motion platform can only move in 1 dimension, the longitudinal direction. In a clinical scenario, patients can shift positions in 6° of freedom. The phantom was set up in the prone position for this study, which differs from the standard supine position of most spine SBRT treatments. By translating the angular data by 180°, the conclusions of this study are still applicable to clinical cases with similar hardware geometry. For hardware tracking spine SBRT cases that occur in the clinic at Ohio State University, multiple triggered images are typically considered to decide if the patient has shifted significantly before pausing treatment. Because the motion of the phantom between triggered images was randomized in phase 1, each image had to be considered separately by the user. In this way, the simulated treatment was different from what typically occurs in a clinical setting. Additionally, the users had no knowledge of where the planned target volume was located, so they had to consider the hardware motion alone when deciding if the shift that occurred was outside of clinical tolerance. It is standard to treat spine SBRT patients in the supine position, but this study was performed with the phantom situated in the prone position. The gantry/OBI angle dependence is another aspect to be evaluated. There is a need for future studies to experiment with the size of the contour to determine the feasibility of

improving detection accuracy. Additionally, clinical users of IMR are encouraged to undergo additional training to enhance their ability to identify shifts larger than clinical tolerance as "out." Positional shifts that occur in dimensions other than the longitudinal direction should also be incorporated to create a study that is more reflective of all degrees of freedom.

Conclusion

Overall, the use of contour-based IMR should be carefully considered when being implemented as a clinical tool for monitoring patient position as applied to spine SBRT cases with hardware. Based on the quantitative data collected by this study, most of the 17 participants independent of their role in the radiation oncology department struggled to detect submillimeter shifts greater than a clinical threshold of 1 mm. User perception sensitivity did not exceed 0.5 until there was a physical shift of 1.4 mm. Therefore, the use of a 1-mm isotropic expansion contour did not show to be a reliable metric to use as a method of tracking shifts between 1.0 and 1.5 mm in magnitude. However, contour-based IMR could still provide beneficial information for larger intrafraction motion during treatment and could be valuable for identifying gross anatomic motion during treatment.

Disclosures

Ashley Cetnar reports financial support by The Ohio State University, a relationship with the American Association of Physicists in Medicine that includes a board membership, and roles as associate senior editor of *Advances in Radiation Oncology* and an associate editor of the *Journal of Applied Clinical Medical Physics*. Erika A. Jank reports a relationship with the American Association of Physicists in Medicine that includes stipend funding.

Supplementary materials

Supplementary material associated with this article can be found in the online version at doi:10.1016/j.adro.2023.101351.

References

1. Redmond KJ, Lo SS, Fisher C, Sahgal A. Postoperative stereotactic body radiation therapy (SBRT) for spine metastases: A critical review to guide practice. *Int J Radiat Oncol Biol Phys*. 2016;95:1414-1428.
2. Koo J, Nardella L, Degnan M, et al. Triggered kV imaging during spine SBRT for intrafraction motion management. *Technol Cancer Res Treat*. 2021;20:15330338211063033.
3. Eckstein J, Koffler D, Parashar B, Potters L, Narayana A. Guidelines for palliative treatment of spinal metastases: Choosing between stereotactic body radiation therapy and conventional fractionation. *Oncology*. 2021;35:63-69.
4. Fan Q, Pham H, Zhang P, Li X, Li T. Evaluation of a proprietary software application for motion monitoring during stereotactic paraspinal treatment. *J Appl Clin Med Phys*. 2022;23:e13594.
5. Amankulor NM, Xu R, Iorgulescu JB, et al. The incidence and patterns of hardware failure after separation surgery in patients with spinal metastatic tumors. *Spine J*. 2014;14:1850-1859.
6. Maranzano E, Bellavita R, Floridi P, et al. Radiation-induced myelopathy in long-term surviving metastatic spinal cord compression patients after hypofractionated radiotherapy: A clinical and magnetic resonance imaging analysis. *Radiother Oncol*. 2001;60:281-288.
7. Ma L, Sahgal A, Hossain S, et al. Nonrandom intrafraction target motions and general strategy for correction of spine stereotactic body radiotherapy. *Int J Radiat Oncol Biol Phys*. 2009;75:1261-1265.
8. Chang Z, Wang Z, Ma J, O'Daniel JC, Kirkpatrick J, Yin FF. 6D image guidance for spinal non-invasive stereotactic body radiation therapy: Comparison between ExacTrac X-ray 6D with kilo-voltage cone-beam CT. *Radiother Oncol*. 2010;95:116-121.
9. Cetnar A, Ayan AS, Graeper G, et al. Prospective dual-surrogate validation study of periodic imaging during treatment for accurately monitoring intrafraction motion of prostate cancer patients. *Radiother Oncol*. 2021;157:40-46.
10. Cetnar A, Degnan M, Pichler J, et al. Implementation of triggered kilovoltage imaging for stereotactic radiotherapy of the spine for patients with spinal fixation hardware. *Phys Imaging Radiat Oncol*. 2023;25:100422.
11. Hancock PA. On the nature of vigilance. *Hum Factors*. 2017;59:35-43.
12. Kaur G, Lehmann J, Greer PB, Martin J, Simpson J. Clinical validation of the Varian Truebeam intra-fraction motion review (IMR) system for prostate treatment guidance. *Phys Eng Sci Med*. 2023;46:131-140.
13. Korpics MC, Rokni M, Degnan M, Aydogan B, Liauw SL, Redler G. Utilizing the TrueBeam Advanced Imaging Package to monitor intrafraction motion with periodic kV imaging and automatic marker detection during VMAT prostate treatments. *J Appl Clin Med Phys*. 2020;21:184-191.
14. Ho AK, Fu D, Cotrutz C, et al. A study of the accuracy of cyberknife spinal radiosurgery using skeletal structure tracking. *Neurosurgery*. 2007;60(2 Suppl 1). ONS147-156.